ELSEVIER

International Journal of Mass Spectrometry 185/186/187 (1999) 589–602

International Journal of Mass Spectrometry

Laser excited N_2^+ in a 22-pole ion trap: experimental studies of rotational relaxation processes

S. Schlemmer*, T. Kuhn, E. Lescop, D. Gerlich

Institute of Physics, Technical University of Chemnitz, 09107 Chemnitz, Germany

Received 22 June 1998; accepted 5 August 1998

Abstract

The laser induced charge transfer $N_2^+ + Ar \rightarrow Ar^+ + N_2$ has been employed to measure rotationally resolved excitation spectra of N_2^+, held in a 22-pole ion trap. Detection of the Ar^+ product ions proved to facilitate an almost background free spectroscopic method. Rotational temperatures and Doppler temperatures determined from these spectra show that the internal and translational degrees of freedom of the parent ions are very well coupled to the trap temperature via collisions with the Ar buffer gas. Laser excitation starts a complex reaction kinetics of the finite ensemble of N_2^+ ions. Various elementary reaction steps have been distinguished and followed in detail by varying laser duration, storage time, and target gas density. For a fixed temperature (90 K), specific rate coefficients have been determined. Pumping only one particular quantum state of ortho-N_2^+ ($X^2\Sigma_g$, $v'' = 0$, $J'' = 6.5$) shows that rate coefficients for the mixing of fine structure states (F_1/F_2) as well as nuclear spin states (ortho/para) in collisions with Ar are negligible (smaller than 10^{-12} cm^3 s^{-1}). The rate coefficient for transitions between the rotational states of one subset, e.g. ortho-N_2^+ (F_1), are surprisingly small. The results are discussed in the framework of possible dynamical constraints, e.g. imposed by the potential energy surface. (Int J Mass Spectrom 185/186/187 (1999) 589–602) © 1999 Elsevier Science B.V.

Keywords: Rotational relaxation; Laser induced charge transfer; Ion traps; Rate coefficients; Fine structure changing collisions

1. Introduction

The acquisition of spectra of molecular ions has been and still is a formidable task to spectroscopists. Because of their transient nature and space charge problems, ions are hard to produce in large enough quantities to obtain a high resolution spectrum in emission or absorption. For some systems, the method of laser induced fluorescence (LIF) has been used successfully. Other laser induced processes such as the opto-acoustical or the opto-galvanic effect pose an interesting alternative. In the first type of experiments, laser excited molecules release their excitation energy via inelastic collisions into translational energy of a buffer gas leading to an acoustic signal. In the second type the discharge current is perturbed by laser induced modifications of the charge distributions. This method can be very sensitive, but usually the involved chemical plasma kinetics are very complicated and only poorly understood. Besides ionization, electron ion recombination, and other processes, laser induced charge transfer is an important elementary step. A prototype example for this is the charge

* Corresponding author.

Dedicated to Professor Michael T. Bowers on the occasion of his 60th birthday.

PII S1387-3806(98)14141-6

transfer (CT) reaction $N_2^+ + Ar \rightarrow Ar^+ + N_2$, occurring for example in an Ar/N_2 discharge.

It has already been demonstrated by Grieman et al. [1] that Ar^+ ions formed by this reaction can be used as a monitor to obtain an excitation spectrum of N_2^+. This reaction system is especially suited as a prototype for a laser induced reaction because the reaction requires additional translational energy for ground state N_2^+ ions whereas it is also rapid at low translational temperatures as soon as the excitation energy exceeds the endothermicity of 0.18 eV [1]. The mentioned experiment [1], performed in a selected ion flow tube (SIFT) apparatus, turned out to be very sensitive. By probing only $\approx 10^4$ cm^{-3} parent ions, a full spectrum of the Meinel band ($A^2\Pi_u$ $v' = 4$, $J' \leftarrow X^2\Sigma_g$ $v'' = 0$, J'') could be recorded. Compared to earlier attempts to employ laser induced reaction [2] the detection efficiency was increased by taking advantage of particle counting and the background was reduced by thermalizing the hot parent ions in the SIFT apparatus to $T = 350$ K [1]. However, due to the short passage time of the ions through the laser, its power had to be fairly high (20 W [1]). In addition, a high target gas density was required (10^{15} cm^{-3} [1]) because the distance of the excitation regime to the extraction hole into the mass analyzer and detector was short. It has been pointed out by the authors that measuring the product yield as a function of target density can reveal the rate coefficient for the laser induced reaction step; however, to our knowledge, no result has been reported. Instead, in another SIFT experiment by Kato et al. [3], LIF has been used to determine state specific charge transfer rate coefficients for the system under consideration, $N_2^+(v = 0–4)$.

Besides flow tube experiments, trapping experiments are well suited for spectroscopic or chemical studies with ions. Mahan and O'Keefe [4] used LIF to record the first negative system ($B\ ^2\Sigma_u \leftarrow X^2\Sigma_g$) of N_2^+ ions confined in a Paul trap. The authors could show that N_2^+ produced by electron impact in the trap had an initial rotational distribution close to room temperature but heat up to several thousand degrees due to collisions with Ar. This heating was attributed to a rapid transfer of translational into rotational energy (T–R transfer). These results indicate that the combination of trapping experiments and laser induced processes can be used to obtain information about the collision dynamics of the molecular system under consideration.

We report here on a different experimental approach employing laser induced reaction as a technique to not only receive spectroscopic information but also to use it for detailed dynamical studies of the various reaction steps involved. A small number of parent ions, typically 2000, is stored in a temperature variable 22-pole rf ion trap in the presence of a low density Ar buffer. In contrast to the experiments in the Paul trap, in this trap all degrees of freedom are thermalized to the temperature of ambient buffer gas. Because of long ion–laser interaction times, 5 mW from a diode laser are sufficient to initiate a significant fraction of the trapped ions to undergo the laser induced CT reaction. Analyzing this product yield as a function of excitation wavelength easily reveals a rovibrational N_2^+ spectrum. Moreover, the parameters determining the product yield can be varied over a wide range. Changing the storage time, rates can be determined at a constant target number density and for a particular initial rovibrational state ($v'' = 0$, J''). Varying the target number density or the laser power, reaction steps involving a collision can be separated from unimolecular steps.

In the following we describe an experiment in which the dynamics of rotational relaxation of the parent ions has primarily been examined. After the experimental section, N_2^+ spectra are presented. These spectra have also been used to determine the translational and rotational temperature of the stored ion cloud. We then describe the determination of the rate coefficients of the relevant kinetic steps. In the discussion we give a simple model to explain that the rotational relaxation process is nonstatistical. Influences of possible fine structures of the potential energy surface of the $(N_2Ar)^+$ system on these processes will be discussed.

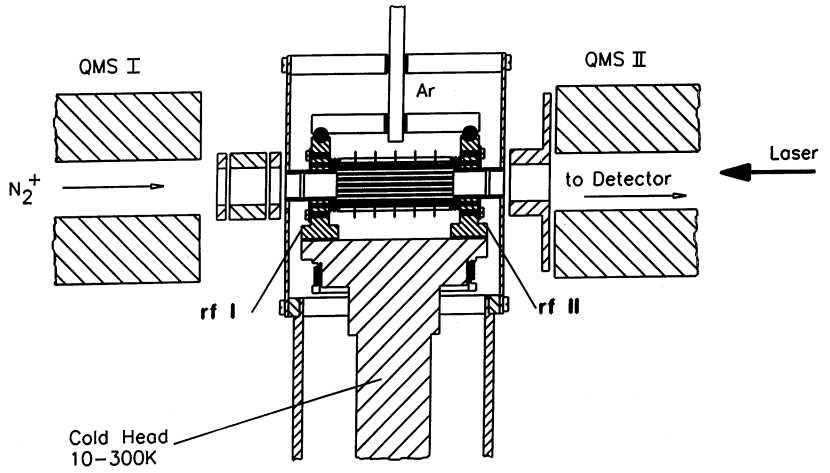

Fig. 1. Schematic view of the ion trap apparatus. N_2^+ primary ions are transferred from the ion source by a quadrupole mass spectrometer (QMS I) into the cooled radio frequency 22-pole ion trap. Reactant ions and formed products are stored for a preset time before extraction, mass analysis in the second quadrupole (QMS II), and detection. During storage N_2^+ can be excited by a collimated diode laser to initiate the charge transfer reaction $N_2^+ + Ar \rightarrow Ar^+ + N_2$.

2. Experimental

2.1. Guided ion beam apparatus/22-pole ion trap

Fig. 1 shows a schematic view of the central part of the experimental setup. The principles of this ion trap apparatus have been described in some detail before [5,6]. In brief, N_2^+ ions are produced by electron bombardment from residual N_2 in a storage ion source, i.e. outside of the 22-pole trap. The mean residence time in this source is on the order of milliseconds; therefore, ions are delivered with an internal temperature close to room temperature. For every trapping cycle a train of ions is extracted into a quadrupole mass spectrometer (QMS I) that selects the N_2^+ ions from the ion beam and transfers them into the 22-pole ion trap. There, they are stored up to minutes by the radial rf field created by the 2×11 stainless-steel rods, and by the electrostatic potential of the entrance and exit orifices. The trap is mounted on the second stage of a closed cycle refrigerator (Leybold, RGD 210). Coupling between the wall temperature and the ion temperature is usually mediated by collisions with the ambient target gas. For the experiments presented in this article, temperatures above 100 K were generally chosen to avoid condensation of the Ar target gas. After a preselected storage time, the ions are extracted from the trap, mass analyzed in another quadrupole mass spectrometer (QMS II), and detected by conventional single ion counting techniques. The trapping cycle is repeated for a variety of storage times and for the reactant or product masses of interest.

Rate coefficients can be determined from the number of parent and product ions as a function of residence time in the trap, together with the accurately determined target gas number density. At pressures in the range of 10^{-5}–10^{-3} mbar, the target gas number density is measured by a spinning rotor gauge (MKS, quoted accuracy $<5\%$). For experiments at lower target gas number densities (trap pressure $p < 10^{-5}$ mbar) an ionization gauge is used. The ion gauge is calibrated by the spinning rotor gauge in the overlapping pressure range. A large contribution to the uncertainty in the target gas number density is because of the density gradient along the trap axis and also the density fluctuations caused by variations of the trap temperature leading to condensation and reevaporation of target gas. For the data analysis we therefore have to use an effective target gas density for which we conservatively estimate an error of $\approx 20\%$.

2.2. Laser system

Previous works in the literature concerning the N_2^+ Meinel band ($A^2\Pi_u \leftarrow X^2\Sigma_g$) have been explored to the extent of accurate transition frequencies, radiative lifetimes, Einstein coefficients, and f values for individual rovibrational lines [7–9]. We have used a 780 nm laser diode (Sharp, LTO26MD0) [10] for optical excitation of the ($A^2\Pi_u$ $v' = 2$, $J' \leftarrow X^2\Sigma_g$ $v'' = 0$, J'') band. This diode, which has a threshold current of ~40 mA, was operated between 50 and 80 mA injection current leading to single mode conditions. Under these conditions, the output power is up to 5 mW. The linewidth is less than 100 MHz. Coarse tuning the laser frequency of the diode is done using an actively driven Peltier element keeping the temperature constant within a very small fraction of a degree in the range between 13–29 °C. Fine tuning and scanning the laser frequency is achieved by variation of the diode current. The typical rate is several GHz/mA. A 2 GHz etalon with a finesse of about 200 (Burleigh) and a 9.8 GHz etalon (homemade) are used for frequency calibration purposes.

3. Results

3.1. Laser induced charge transfer (LICT)

The laser excitation and collisional processes involved in the present study of N_2^+ + Ar collisions are illustrated in Fig. 2. It shows a schematic energy level diagram of N_2^+ in its electronic ground state ($X^2\Sigma_g$, v'' = 0, J''), one particular J' level of the excited $A^2\Pi_u(v' = 2)$ state, and the $Ar^+(^2P_J)$ product state. Because of the endothermicity of 0.18 eV, the CT rate coefficient

$$N_2^+(v'' = 0) + Ar \rightarrow Ar^+(^2P_J) + N_2 \quad (1a)$$

is very small at room temperature, $k_{CT}(v = 0) < 10^{-12}$ cm^3 s^{-1} [11,12]. However, it has been shown by various authors [1,12] that vibrationally excited N_2^+ reacts with a considerably larger charge transfer rate coefficient $k_{CT}(v > 0) = 4 \times 10^{-10}$ cm^3 s^{-1}

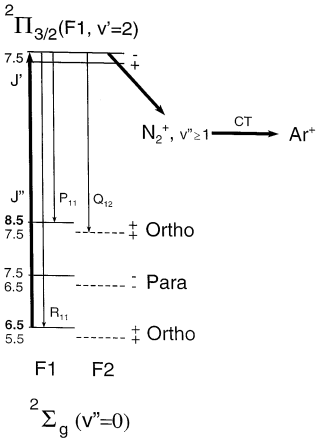

Fig. 2. Schematic level diagram of N_2^+ with those reaction pathways that are relevant for the present experiment. Ortho-N_2^+ in its electronic ground state level ($X^2\Sigma_g$, $v'' = 0$, $J'' = 6.5$, F_1) is laser excited to $A^2\Pi_u(v' = 2, J' = 7.5)$ (excitation rate: R_{abs}). Fluorescence of this state populates either o-N_2^+ ($v'' > 0$, J''), which has sufficient energy to undergo charge transfer with Ar^+ (rate coefficient: k_{CT}) or o-N_2^+ ($v'' = 0$, $J'' = 6.5$, 7.5, and 8.5). The laser driven change of the rotational state population of o-N_2^+ is thermalized by inelastic collisions with the Ar buffer gas (rate coefficient: $k_{N\rightarrow N'}$, N denotes the rotational quantum number) not shown as arrows for clarity.

$$N_2^+(v'' > 0) + Ar \rightarrow Ar^+(^2P_J) + N_2 \quad (1b)$$

As a consequence, detection of Ar^+ from the charge transfer reaction can be used as a very sensitive monitor for the presence of vibrationally excited N_2^+. Without laser excitation, the trapped N_2^+ ions remain in their vibrational ground state and practically no Ar^+ ions are formed in the trap. When the laser hits the $A^2\Pi_u(v' = 2, J') \leftarrow X^2\Sigma_g(v'' = 0, J'')$ transition, about 55% of all laser excited N_2^+ molecules fluoresce into vibrational levels $v'' \geq 1$ in the present experiment (see Fig. 2). Thus the detection of Ar^+ indicates the laser excitation of N_2^+, and the Ar^+ ion signal versus the wavelength can be used to record a spectrum of N_2^+. As already mentioned in the introduction, this method has been employed previously [1] in a flow tube experiment to determine the optical spectrum of $A^2\Pi_u(v' = 4, J') \leftarrow X^2\Sigma_g(v'' = 0, J'')$. In the present trap experiment much smaller number densities are needed to record such a spectrum.

Fig. 3 shows the band head of the R_{11} branch of the

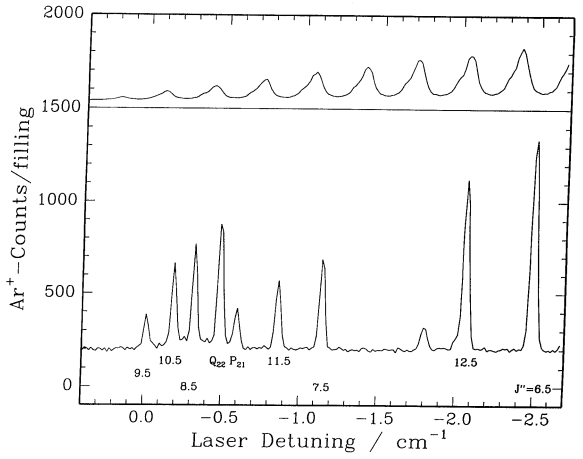

Fig. 3. Variation of the laser frequency in the region of the band head of the R_{11} branch of the N_2^+ [$A^2\Pi_u(v' = 2) \leftarrow X^2\Sigma_g(v'' = 0)$] transition. The temperature stabilized diode laser is tuned by scanning the injection current of the diode. *Upper trace*: Fringes of a 9.8 GHz etalon used for frequency calibration. *Lower trace*: Ar^+ ions from laser induced charge transfer are used as a monitor for detection of the spectrum.

$A^2\Pi_u(v' = 2, J') \leftarrow X^2\Sigma_g(v'' = 0, J'')$ transition. For each point of the spectrum only about 2000 N_2^+ parent ions were stored for 200 ms in the trap during continuous irradiation with the laser diode. The plotted spectrum, which was taken at room temperature, is an average of five scans. Most lines in this spectrum belong to the progression of the R_{11} branch, marked by the rotational levels $J'' = 6.5$–12.5. The upper portion of Fig. 3 shows the fringes of the 9.8 GHz etalon that have been recorded as a second trace. Both signals have not been corrected for the laser intensity varying with the detuning. Because the diode laser output power is proportional to the injection current above threshold, it also increases more or less linearly with the detuning. This can be seen from the etalon scan. To obtain the correct absorption signal (and for other quantitative evaluations) the observed Ar^+ signal has been normalized to the actual measured laser power.

3.2. Characterization of the stored N_2^+ ions

Trapping experiments are widely used for the determination of thermal rate coefficients for ion–molecule reactions [13]. The use of higher order multipole rf traps made it possible to obtain rate coefficients down to fairly low temperatures ($T \geq 10$ K) [5,6]. However, there has been a long debate as to what extent the trapped ions reach the wall temperature [6,13,14]. In the present experiment we have examined the rotational and one translational degree of freedom of the stored ions.

From a measured spectrum of N_2^+ the rotational population of the trapped N_2^+ ion cloud has been calculated using the following procedure. The rotational lines of the R_{11} branch in Fig. 3 originate from the electronic fine structure component F_1 ($J'' = N'' + 1/2$) of ground state N_2^+ in its two nuclear spin components o-N_2^+ ($N = 0, 2, 4\ldots$) and p-N_2^+ ($N = 1, 3, 5\ldots$). The ion signal, after correction for the laser power, is proportional to the degeneracy of the nuclear spin configurations, g, to the Hönl–London factors, $S(J'')$, and the population probability of the initial states. For the $^2\Pi \leftarrow {}^2\Sigma$ transitions we have calculated the Hönl–London factors using the formulas given by Earls [15]. Under thermal conditions, the population of the rotational states in the X state would be given by the Boltzmann factor, $\exp(-E_{rot}/kT)$ with $E_{rot} = hcB''(J'' - 1/2)(J'' + 1/2)$. Note that the multiplicity of the total angular momentum J'' has already been accounted for by the Hönl–London factor. In order to test the measured population and to extract a temperature, the rotational state distribution for the R_{11} branch has been displayed in a Boltzmann plot, e.g. following the expression

$$\ln [I/gS(J'')] = -E_{rot}/kT + \text{const}$$

Fig. 4 shows such a plot for a spectrum taken at a nominal temperature of 120 K. The rotational temperature determined from a linear regression is (126 ± 6) K, which is in excellent accordance with the nominal temperature defined by the walls of the trap.

In order to determine the translational temperature of the ion cloud, the line shape of several rovibrational transitions was recorded at a smaller frequency step size and fitted with a Gaussian function, accounting for the Doppler profile caused by the ion motion. Fig. 5 shows two such rotational lines with their

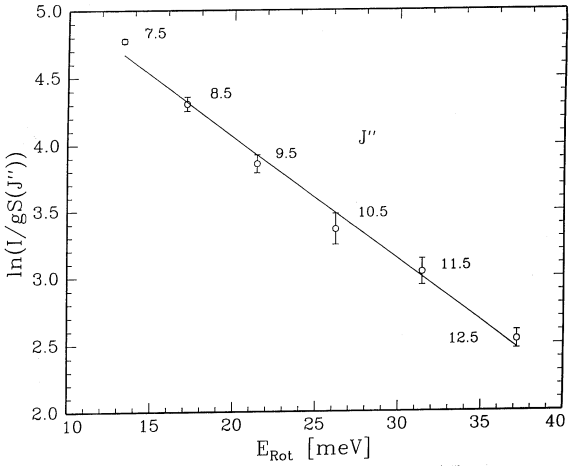

Fig. 4. Determination of the rotational temperature of N_2^+ from a Boltzmann plot. The logarithm of the measured intensities, which have been corrected for the laser power and divided by the nuclear spin multiplicities (g) and the Hönl–London factors $S(J'')$, are obviously close to a thermal population. The linear regression leads to a rotational temperature, $T = (126 \pm 6)$ K that is in good agreement with the nominal temperature of the trap.

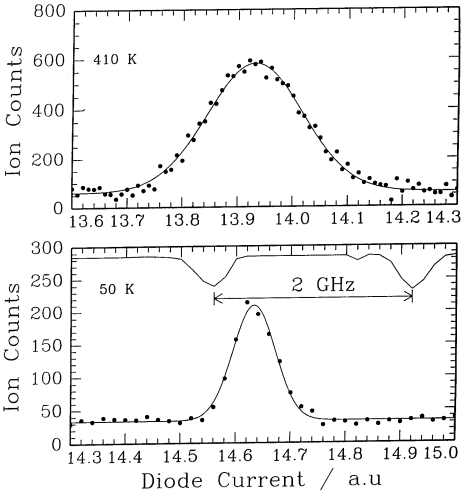

Fig. 5. Doppler profiles of a specific laser transition at two temperatures (wall temperature of the trap, upper panel: (400 ± 30) K, lower panel: (50 ± 10) K). In good agreement with these nominal temperatures, the fitted Maxwell Boltzmann distributions (solid lines) result in translational temperatures of 410 and 50 K, respectively. For frequency calibration purposes fringes of a 2 GHz Etalon are recorded as a second trace.

respective fits. The temperature of the fitted Maxwell–Boltzmann velocity distributions are in good overall agreement with the nominal temperature of the trap (see Fig. 5 caption). The 2 GHz etalon fringes routinely used for frequency calibration are included in the lower panel. Such experiments have been repeated at various nominal temperatures and good overall agreement was found.

As a critical test, the two measured temperatures can be compared with each other. As an example, Fig. 6 shows the translational temperature (for $J'' = 7.5$) as a function of the rotational temperature derived from all measured J''. Although the scatter in these measurements is fairly large (30 K), it can be seen, that T_{trans} versus T_{rot} follows very well the expected straight line at 45°. However, the linear regression indicates that the measured translational temperature may be slightly lower than the rotational temperature. This can be qualitatively explained by the fact that our measurements are performed with a very limited number of ions. Even at comparably short times for laser excitation, inelastic scattering may couple translation and the rotational states sufficiently that the thermal equilibrium of the very small ensemble is perturbed. This obviously can lead to differences in the two apparent temperatures, T_{trans} and T_{rot}. Disregarding these subtleties, which will be discussed in more detail in the next section, we take the extensive

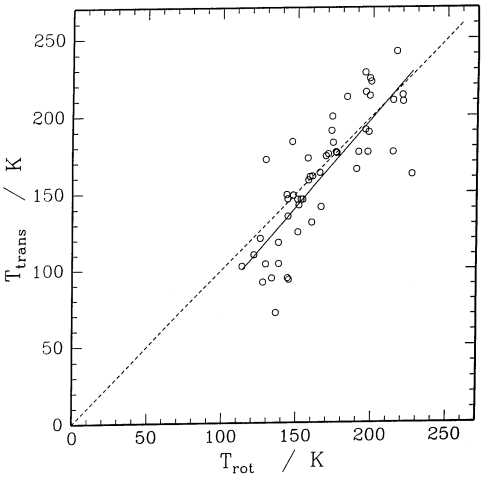

Fig. 6. Comparison of the translational and rotational temperature over a range from 100–250 K. The translational temperatures has been derived from the Doppler profile of the $J'' = 7.5$ line.

temperature measurements as a good indication that in our multipole ion trap, the ion temperature is well adjusted to the wall temperature by collisions with the "heat bath" molecules.

4. Dynamical processes

4.1. Kinetic time scales

In the previous section the production of Ar^+ ions was simply used as a monitor for vibrationally excited N_2^+ without further investigation of the temporal evolution of their appearance. However, trap experiments are perfectly suited to unravel the various dynamical processes involved in their production. Indeed, the processes at work in the LICT experiment are quite complicated, as indicated in Fig. 2. In the following, the rate equation system for a variety of involved steps is described in the order of appearance in the scheme of Fig. 2. As we will show, several experimental parameters are at hand to separate the kinetic time scales of the observable processes. This leads to a quantitative determination of different rate coefficients that will be discussed in the next section.

For the description, we start the kinetics with the laser excitation process that depopulates one particular rovibrational ground state level. For the purpose of observing this influence, the laser wavelength is kept constant, pumping a well defined initial state $i = (F_1, v'' = 0, J'' = 6.5)$ of $o\text{-}N_2^+(X)$ into a final state, $f = (F_1, v' = 2, J' = 7.5)$ of $o\text{-}N_2^+(A)$, see Fig. 2, at a rate of

$$R_{\text{abs}} = B_{i\to f}\rho. \tag{2}$$

Here, $B_{i\to f}$ is the Einstein coefficient and ρ is the spectral energy density of the laser

$$\rho = P/(A_{\text{eff}} c \Delta\nu), \tag{3}$$

with P the laser power (running single mode), A_{eff} its effective cross sectional area [16] and $\Delta\nu$ its effective linewidth [16]. The Einstein coefficient for absorption, $B_{i\to f}$, can be expressed by the Einstein coefficient for emission, $A_{f\to i}$

$$B_{i\to f} = c^3/(8\pi h\nu^3)\, A_{f\to i} \tag{4}$$

Here c is the speed of light, h is Planck's constant, and ν is the excitation frequency. $A_{f\to i}$ is related to the radiative lifetime ($\tau_f = 10\ \mu$s [8]) of the excited state f by

$$\tau_f^{-1} = \sum_i A_{f\to i} \tag{5}$$

Taking into account the appropriate Franck–Condon and Hönl–London factors for the transition under consideration (see Fig. 2), Eq. 2 can be rewritten as

$$R_{\text{abs}} = 0.097 c^2 P/(8\pi h\nu^3 A_{\text{eff}}\Delta\nu). \tag{6}$$

For the transition of interest, the laser power of 3 mW transmitted trough the trap leads to a typical excitation rate of $R_{\text{abs}} \approx 130\ \text{s}^{-1}$ at a Doppler temperature of 100 K. This rate, together with other important rate coefficients is summarized in Table 1.

The excited state decays at a rate $\tau_f^{-1} = 10^5\ \text{s}^{-1}$ [8] into various vibrational levels of the electronic ground state of N_2^+. In this way 45% of the ions are returning back into the vibrational ground state populating those J'' levels which are plotted in Fig. 2. The corresponding relative vibrational and rotational transition probabilities are given in Table 1. They were taken from [8] and calculated from the Hönl–London factors using the formula given in [15], respectively. The remaining 55% become vibrationally excited. As indicated in the diagram of Fig. 2, they are all assumed to undergo charge transfer according to Eq. 1(b), because inelastic processes seem to play only a minor role. This assumption is supported by an experiment by Kato et al. [17,18] who found that the rate for vibrational quenching

$$N_2^+(v'') + \text{Ar} \rightarrow N_2^+(v \neq v'') + \text{Ar} \tag{7}$$

is rather small, $k_v < 1.2 \times 10^{-11}\ \text{cm}^3\ \text{s}^{-1}$.

Up to this point in the discussion, the disappearance kinetics of N_2^+ was determined by two steps: first laser excitation, which is independent on the Ar target gas density, and then charge transfer, the rate of which is proportional to the target gas density. This fact is illustrated in the experimental results shown in Fig. 7. The top and bottom panel show the normalized N_2^+

Table 1
Summary of the relevant rates for laser excitation, radiative decay, and rate coefficients in N_2^+ + Ar collisions. The relative vibrational transition probabilities are taken from [8]. The relative rotational transition probabilities are calculated from the Hönl–London factors, see formulas given in [15]

			Rate/rate coefficient		
Process	Symbol	Eq.	Previous work	Ref.	This work
Laser excitation	R_{abs}	6			$(130 \pm 25)\ s^{-1}$
Radiative decay	τ_f^{-1}	5	$10^5\ s^{-1}$	[8]	
Charge transfer	$k_{CT}(v'' = 0)$	1a	$<10^{-12}\ cm^3\ s^{-1}$	[11]	
Coefficient	$k_{CT}(v'' > 0)$	1b	$4 \times 10^{-10}\ cm^3\ s^{-1}$	[3]	$(4 \pm 2) \times 10^{-10}\ cm^3/s$
Vibrational quenching	k_v	7	$<1.2 \times 10^{-11}\ cm^3\ s^{-1}$	[17]	
Rotational relaxation	k_J	10			$(1.4 \pm 0.4) \times 10^{-11}\ cm^3\ s^{-1}$
Complex formation	k_C	16			$8.5 \times 10^{-12}\ cm^3\ s^{-1}$
Langevin rate coefficient	k_L	13	$7.4 \times 10^{-10}\ cm^3\ s^{-1}$		
Vibrational transition probabilities					
$P(v' = 2 \rightarrow v'' = 0)$	0.45				
$P(v' = 2 \rightarrow v'' \geq 0)$	0.55				
Rotational transition probabilities					
$P(F_1, v' = 2, J' = 7.5 \rightarrow F_1, v'' = 0, J'' = 6.5)$	0.38				
$P(F_1, v' = 2, J' = 7.5 \rightarrow F_1, v'' = 0, J'' = 8.5)$	0.28				
$P(F_1, v' = 2, J' = 7.5 \rightarrow F_2, v'' = 0, J'' = 7.5)$	0.33				

counts as a function of storage time. After a thermalizing trapping period of a few milliseconds (not included in Fig. 7) the laser was tuned on resonance for a period of 10 ms. In the upper panel the N_2^+ counts show a steep decrease by 3.5% within the period of laser excitation and stay constant immediately after the laser is switched off. For this measurement the Ar number density was $2.5 \times 10^{12}\ cm^{-3}$. Obviously, this target gas density is high enough that all vibrationally excited N_2^+ ions are undergoing charge transfer on a time scale shorter than the time scale for laser excitation. In the lower panel N_2^+ disappears on a longer time scale. Here the Ar number density was ten times lower, $2.5 \times 10^{11}\ cm^{-3}$. In this case the time scales for the two processes become comparable. Therefore, the number of N_2^+ counts is decreasing slower, and even after the laser is tuned of resonance this number still decays because there are still some vibrationally excited N_2^+ ions left.

The solid lines in both graphs of Fig. 7 are the result of a computer simulation solving the coupled rate equation system including laser excitation, R_{abs}, fluorescence, τ_f^{-1}, charge transfer, $k_{CT}(v > 0)$, and rotational relaxation k_J. The simulations fit both experimental data sets very well with one set of parameters, $R_{abs} \approx (130 \pm 25)\ s^{-1}$, $\tau_f^{-1} = 10^5\ s^{-1}$, $k_{CT}(v > 0) = (4 \pm 2) \times 10^{-10}\ cm^3\ s^{-1}$, and $k_J = 1.2 \times 10^{-11}\ cm^3\ s^{-1}$. Despite this good agreement, the estimated errors for laser excitation (20%) and charge transfer (50%) are fairly large. This is because of the rather weak sensitivity of the quality of the fit to the four kinetic parameters. The reproducibility of the experiments is better than these errors indicate. Comparison of our results to previous experiments [11,12] reveals a very similar value for the charge transfer rate of $N_2^+(v'' > 0)$. In addition, the rate for laser excitation agrees well with the expected value using Eq. 6.

4.2. Thermal evolution

The laser excitation followed by fluorescence is changing the thermal distribution of rotational states of our limited ensemble of N_2^+ ions. The first obvious

effect is a depopulation of the particularly pumped rotational state, N''. This mechanism has been taken into account for the simulations displayed in Fig. 7 and will be considered in greater detail in the following. At thermal and higher energies rotational relaxation

$$N_2^+(v'', N'') + Ar \rightarrow N_2^+(v'', N) + Ar \quad (8)$$

is thought to be a rather fast process. However, the value deduced from the above simulation ($k_J = 1.2 \times 10^{-11}$ cm^3 s^{-1}) is rather small compared to the Langevin rate coefficient, $k_L = 7.4 \times 10^{-10}$ cm^3 s^{-1}. Therefore, much longer times than those used in Fig. 7. have to be considered if one wants to observe an influence of rotational redistribution.

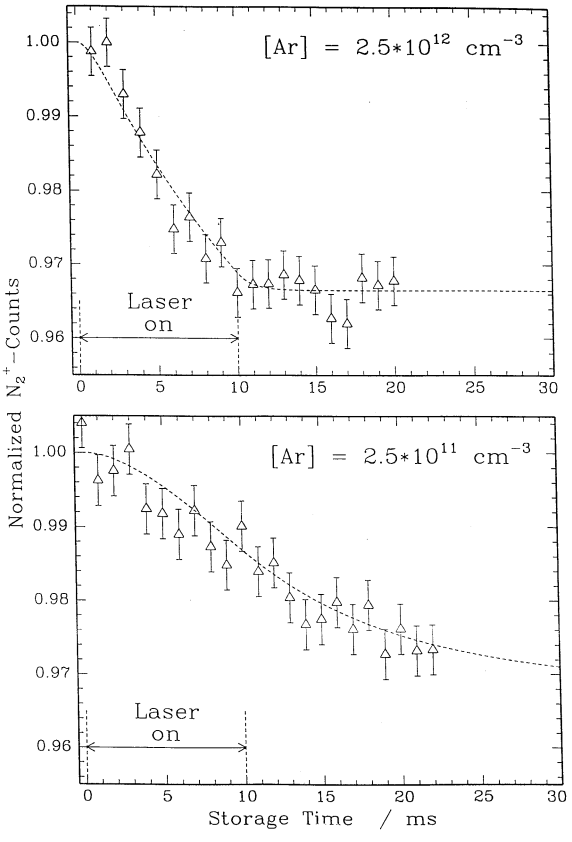

Fig. 7. Relative number of N_2^+ parent ions during and after a laser excitation of 10 ms. *Upper panel*: [Ar] = 2.5 × 10^{12} cm^{-3}. No depletion after laser excitation. Charge transfer (rate: k_{CT} × [Ar]) is more rapid than laser excitation (rate: R_{abs}). *Lower panel*: [Ar] = 2.5 × 10^{11} cm^{-3}. Further depletion after laser excitation. Laser excitation and charge transfer are happening at a comparable rate. Solid lines are a numerical simulation; results are summarized in Table 1.

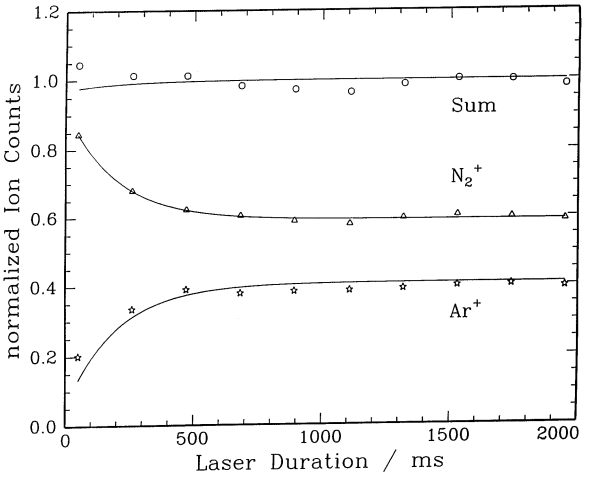

Fig. 8. Normalized number of N_2^+ and Ar^+ as a function of laser duration (T = 90 K, [Ar] = 4.4 × 10^{12} cm^{-3}). All ions are stored for 2 s. N_2^+ is only fractionally depleted by about 40% within the first second. Solid lines represent a numerical simulation of the experiment. Best fit results reveal that more than 50 collisions are necessary for rotational relaxation.

Fig. 8 shows an experimental result where an initial ensemble of N_2^+ ions is trapped for a total of 2 s under constant conditions with the exception that the excitation laser is switched on for a time varying between 50 and 1950 ms. Inspection shows that for short excitation times only a small fraction of the N_2^+ ions is converted into Ar^+ ions, whereas for long irradiation, about 40% of the injected N_2^+ undergo CT and produce Ar^+ ions. At the Ar target gas number density of this measurement, 4.4 × 10^{12} cm^{-3}, the number of N_2^+ remains unchanged after about 1 s. Note that, for all laser durations, the sum of N_2^+ and Ar^+ ions is constant within the statistical fluctuations. This verifies that N_2^+ is only transformed by LICT to Ar^+ and that no other loss mechanisms have to be accounted for.

In order to understand the experimentally observed conversion rate one has to note that the laser interacts exclusively with those N_2^+ which are in the $J'' = 6.5$ (F_1, $N'' = 6$) state and that only about 8% are in this state if the initial population is in thermal equilibrium.

The observed larger reduction of N_2^+, 40%, shows that rotational redistribution plays a role, whereas the fact that a major fraction remains unperturbed is an indication that many N_2^+ ions of the ensemble cannot be converted into the state pumped by the laser. It appears safe to assume that all those N_2^+ ions that are in the F_1 state of o-N_2^+ can be collisionally converted to the $J'' = 6.5$ (F_1, $N'' = 6$) state and, after laser excitation, into Ar^+. This class accounts for about 38% at $T = 100$ K. Another fraction (about 29%) of the ion cloud is populating the other fine structure state of o-N_2^+, F_2. Since we use normal N_2 in the ion source, both populations must add up to 2/3 of the total N_2^+ ensemble. At elevated temperatures the two fine structure states have a population of 1/3 each, but at the low temperatures of our experiment the fact that F_1, $N'' = 0$ is the lowest lying state leads to a disparity of 0.38/0.29. The remaining fraction, 1/3, is populating both fine structure states of the other nuclear spin state, p-N_2^+.

Without further analysis and accounting for the uncertainty of the conversion rate of a few percent, our experimental observation leads to the important conclusion that neither fine structure state changing collisions nor nuclear spin state changing collisions occur with a significant rate at the conditions of our experiment and that we see predominantly the complete depopulation of F_1 o-N_2^+. For a more quantitative analysis we have to account for two possible experimental problems. One is that some initially hot N_2^+ ions contribute slightly to the 40% Ar^+ products. The other is that some nitrogen gas penetrates from the ion source into the trap and that some N_2^+ ions may undergo CT with these molecules. The CT reaction $^{15}N_2^+$ ($v'' = 0$) + $^{14}N_2$ was found by Frost et al. to proceed at half the Langevin collision rate [19]. It is more probable that such collisions lead to a coupling of the fine structure or nuclear spin states than collisions with Ar. In general we can conclude that the rate coefficients for para-ortho or F_2–F_1 transitions in collisions with Ar are even smaller than the one for rotational relaxation, i.e. $k_{\text{para}\rightarrow\text{ortho}}$, k ($F_2 \rightarrow F_1$) $< 10^{-12}$ cm^3 s^{-1}.

For the experiment presented in Fig. 8 the kinetics has also been simulated and the result is shown by the solid lines. Taking the rate coefficient for charge transfer and the rate of laser excitation from the short time experiments explained above (Fig. 7) such fits have been used to derive information for rotational relaxation of the ions. For simplicity we first define an effective rate coefficient, k_J, in which the influence of the collisions is treated as a net sum of all possible ways of depopulating N'' by $N'' \rightarrow N$ transitions, $N = 0, 2, 4, \ldots$

$$k_J = \sum_{N \neq N''} (k_{N''\rightarrow N}) \tag{9}$$

The value k_J describes the conversion probability of one preselected state J into all other states. Microscopic reversibility connects this rate coefficient with the complementary value that describes the refilling of a hole burned into a thermal distribution. This refilling of the hole is the rate determining step of the complex set of coupled rate equations. In Fig. 8, N_2^+ ions disappear at a rate of about 5 s^{-1}. With $n = 4.4 \times 10^{12}$ cm^{-3} this corresponds to an effective rate coefficient of 1.1×10^{-12} cm^3 s^{-1}. However, the hole is only effectively refilled by a few neighboring states that have a population, $p(N)$, on the order of a few percent up to about 20%, assuming a thermal distribution. The net rate coefficient is the sum of these few and rather small contributions, $k_{N\rightarrow N''} \times p(N)$. Therefore, the individual rate coefficient is considerably larger than this effective rate coefficient. Based on the model given in Eq. 9 we have evaluated experimental results as shown in Fig. 8. The average over several runs, performed under different conditions at a fixed nominal temperature of 90 K leads to the very surprising result that ions in the preselected rotational $J = 6.5$ state undergo changes only with a very small rate coefficient,

$$k_J\,(90\text{ K}) = (1.4 \pm 0.4) \times 10^{-11}\text{ cm}^3\text{ s}^{-1} \tag{10}$$

Comparing this value to the Langevin rate coefficient (see Table 1) implies that only one out of 50 collisions results in a change of the rotational state. This result is unexpected because $(N_2Ar)^+$ can form a strongly bound intermediate molecule with a binding energy of 1.109 eV [20]. Therefore, collision processes should proceed via a long-lived complex at the total energies of

our experiment (meV regime). This usually leads to a statistical mixing of all accessible product channels N_2^+ (J) + Ar. Without any dynamical restrictions at work, rotational redistribution should occur almost at the collision rate! In the following section, the implications of the experimental result will be discussed in more detail.

5. Discussion

5.1. Modelling the rotational relaxation of N_2^+

The first part of a low energy collision, i.e. the approach of the two reactants and the possible formation of a collision complex, is governed by the long range interaction potential. In the case of neutrals, barriers often hinder the approach of the reactants, whereas for ion molecule collisions it is usually assumed that the potential is predominantly attractive. Ignoring fine structure interactions, we first assume for the N_2^+ + Ar system the dominance of the charge induced dipole interaction

$$V_{\text{eff}}(\ell, R) = -\alpha q^2/2R^4 + \ell(\ell+1)\hbar^2/2\mu R^2, \quad (11)$$

where α is the electric dipole polarizability of the neutral collision partner, q is the charge of the ion, R is the distance between the reactants, ℓ is the quantum number of the orbital angular momentum, and μ is the reduced mass of the collision system. According to the Langevin model, a collision complex is formed at a collision energy E_T for all ℓ, for which the centrifugal barrier can be overcome, i.e. for $V_{\text{eff}}(\ell, R) < E_T$. This determines a maximum orbital angular quantum number, $\ell_{\max}$, a maximum impact parameter, $b_{\max}$, and a corresponding cross section

$$\sigma_L = \pi b_{\max}^2 \quad (12)$$

From this Langevin cross section, the corresponding thermal rate coefficient

$$k_L = 2\pi q\,(\alpha/\mu)^{1/2} \quad (13)$$

can also be derived. With $\alpha_{\text{Ar}} = 1.64$ Å^3 we obtain the value for k_L given in Table 1.

If a complex has been formed, the second part of the collision is determined by its decay. Here the outcome may depend on the lifetime, the strength of the interaction, "hidden" constants of motion, or on other possible dynamical restrictions, e.g. barriers in the exit channel. In the past, we have successfully used dynamically biased statistical theories to describe the reaction dynamics of ion–molecule reactions [21,22]. Such theories can be used easily to calculate branching ratios and product state distributions as needed in the present case. At very low collision energies or if light species are involved (small μ), a quantal treatment may become necessary, especially when the number of accessible quantum states is small. However, the N_2^+ + Ar system under consideration here (100 K $< T <$ 150 K, $\mu = 16.47$) behaves fairly classically. The $\ell_{\max}$ involved ($\ell_{\max} \approx 70$) is much larger than the rotational angular quantum numbers, N, of the N_2^+ reactant (most probably $N \approx 4$). This implies that the total angular momentum, J, is dominated by the orbital angular momentum of the relative motion, ℓ,

$$J \approx \ell,\ \ell \gg N,\ \ell' \approx \ell \quad (14)$$

where ℓ' is the value after the collision. As a consequence, the conservation of the total orbital angular momentum does not put significant restrictions on the statistical population of the rotational states of the products.

It has been shown that in the case of two or three identical atoms, conservation of total nuclear spin leads to (approximate) constants of the motion. Our experimental observation that there are no ortho-para transitions is consistent with this fact. This finding can be expressed as the selection rule $\Delta N = 0, 2, 4, \ldots$. Besides this result we see no real restriction for a collision induced rotational transition. Based on these considerations, we are convinced that no simple statistical model can explain our result that rotational transitions in N_2^+ + Ar collisions are almost forbidden.

In order to corroborate this conclusion somewhat quantitatively we present in the following a simple estimate based on a microcanonical equilibrium distribution "with memory" [23]

$$P_0(J''; J) \sim (2J'' + 1)\,(E_{\text{tot}} - E''_{\text{rot}})^{1/2} \quad (15)$$

From this distribution we can derive a thermal, but rotationally state specific distribution $\langle P_0(J''; J)\rangle_T$ by averaging over a thermal distribution of translational energies. Inspection of this expression, which has been calculated numerically, shows that one collision already leads to a rather wide population of product states. In other words, the depopulation probability of an initial state, p_J, is very large. For the initial state $J = 6.5$ we obtain at 100 K the result $p_{6.5} = (1 - \langle P_0(6.5, 6.5)\rangle_{T=100\,\text{K}}) = 0.73$. This large conversion probability is in accordance with the above mentioned fact that any statistical assumption leads to an efficient mixing of all rotational states that are energetically accessible. Therefore, in order to apply this model to the description of our experimental observations we have to introduce a complex formation rate coefficient k_C, that is significantly smaller than k_L. With this assumption, the rate coefficient for a $N \rightarrow N''$ transition can be written as

$$k_{N\rightarrow N''} = k_C\langle P_0(N''; N)\rangle_T \quad (16)$$

In contrast to the information obtained from the experimental results in Fig. 8, this model can be used to predict in detail the temporal evolution of individual N_2^+ rotational states, including both the interaction with the photons and the collisions. The influence of laser excitation and fluorescence alone (i.e. excluding collisions resulting in rotational mixing) is illustrated by the calculated curve in Fig. 9(a). This figure shows the temporal evolution of the population of several states, starting initially from a thermal N_2^+ population, and pumping the $J'' = 6.5$ state by the laser. Its initial population of about 8% disappears within less than 30 ms. Fluorescence is populating $J'' = 8.5$ of the F_1 electronic state and $J'' = 7.5$ of the F_2 electronic state of ortho-N_2^+ which both show a slight increase. The total population in F_1 decreases because of the loss into the F_2 state and because of vibrationally excited N_2^+ undergoing CT with Ar. After 30 ms no significant change in population occurs any longer.

In Fig. 9(b) rotational relaxation is accounted for by including $k_{N\rightarrow N''}$ into the coupled rate equation system. Now, the temporal evolution of the initial thermal distribution extends over a wider time scale.

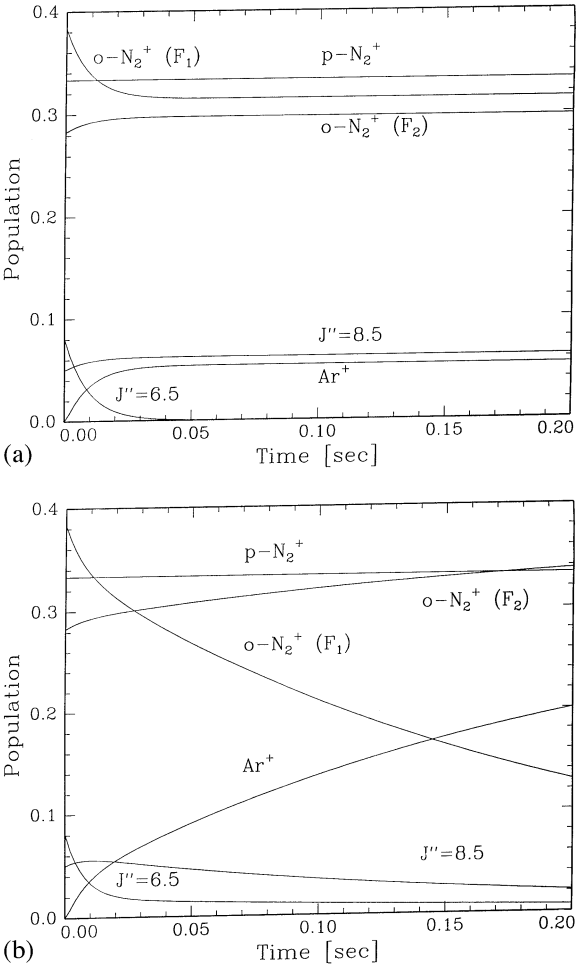

Fig. 9. Numerical simulation. *Upper panel*: Kinetics of the finite population of cold N_2^+ ions, $T = 100$ K, under the influence of the laser pumping $J'' = 6.5$ of the ortho-F_1 subset [$R_{\text{abs}} = 130\ \text{s}^{-1}$], and CT reaction with Ar, [Ar] = $4.4 \times 10^{12}\ \text{cm}^{-3}$. Without allowing rotational mixing, only the 8% population of the initial state disappear within the first ~30 ms, although the laser is on at all times. Only 6% of all N_2^+ ions are undergoing CT with Ar^+. *Lower panel*: Full kinetic simulation including collisions changing the rotational state of ground state N_2^+. All other parameters are as in the upper panel. The rate of disappearance of *o*-N_2^+ (F_1) is comparable to the rate of the experiment (see Fig. 8), $5\ \text{s}^{-1}$. This corresponds to a surprisingly small rate coefficient of rotational relaxation at $8.5 \times 10^{-12}\ \text{cm}^3\ \text{s}^{-1}$.

The $J'' = 6.5$ population shows an initial fast decay in agreement with the results of Fig. 9(a). The subsequent slower decay is mainly determined by those processes which refill the population of the $J'' = 6.5$ state. In contrast to Fig. 9(a), the population of J''

$= 8.5$ is also now decreasing after the initial increase. The F_2 population of ortho-N_2^+ and Ar^+ is increasing accordingly until the F_1 population is completely depleted via the gateway $J'' = 6.5$ and is finally either converted to ortho-$N_2^+(F_2)$ or lost due to Ar^+ CT. As a net result the initial F_1 population of ortho-N_2^+ (~38%) is lost via the latter channel.

In the simulation shown in Fig. 9(b), the decay of the N_2^+ ions has been adjusted to the measured evolution displayed in Fig. 8, by choosing $k_C = 8.5 \times 10^{-12}$ cm^3 s^{-1}. Comparison of the value $k_C \times p_{6.5} = 6.2 \times 10^{-12}$ cm^3 s^{-1} with k_J given in Eq. 10 shows that the more detailed kinetic simulation gives an even smaller rate coefficient than the initial analysis that treated the relaxation as a net effect. The results plotted in Fig. 9(b) show that more detailed experimental information can be obtained if, in a future experiment, the temporal changes are followed experimentally in more detail.

Two questions remain. Is the near conservation of the initial rotational state a consequence of some hidden constants of the motion leading to approximate selection rules or is the complex formation rate coefficient, k_C, really only a few percent of the Langevin value? Concerning the first question, we do not get a clear hint from the calculated potential energy surface; also, the weak anisotropy of the overall attractive potential is very unlikely to play a significant role in conserving the asymptotic rotational state via an intermediate libration. However, barriers in the potential energy surface, in addition to the centrifugal repulsion, could restrict the formation of a collision complex. At the low collision energies of the present work repulsive walls of a few meV are already sufficient to lead to a significant decrease of the capture rate coefficient. In the PES calculations, performed so far for the $(N_2 - Ar)^+$ system [24], no such barriers have been found. Nonetheless, it can be speculated that the inclusion of coupling between electron spin and electron angular momentum (fine structure) or between the motions of electrons and nuclei leads to adiabatic surfaces that are characterized by a switchyard of avoided crossings. Detailed ab initio calculations and quantum mechanical treatment of the collision dynamics at meV energies are required to conclusively answer the questions.

6. Conclusions

In this experimental investigation we showed that the combination of the trapping technique and laser induced reactions provides a sensitive tool to obtain spectroscopic data for ions. The technique is essentially background free for systems that do not react without initial excitation. In the present example, $N_2^+ + Ar$, excitation with visible laser photons was used to overcome the endoergicity of the CT reaction. Searching for suitable reactions, this spectroscopic method may be used for a large class of molecular ions for which no reliable spectroscopic gas phase data are available. The extension of this method to the low temperatures accessible with our trap opens up the field of infrared spectroscopy and allows us to utilize reactions that are only slightly endoergic, e.g. by differences in zero point energy or that are hindered by a small barrier. A candidate for such a study is the $C_2H_2^+ - H_2$ system that is known to produce $C_2H_3^+$ at elevated temperatures whereas it is hindered at the low collision energies accessible in our 22-pole trap [25].

Even more important than obtaining spectroscopic data, the combination of the laser induced reactions with ion trapping proved to be a very versatile tool to investigate state specific details of low temperature ion molecule collisions. Here we found that the two nuclear spin state configurations, ortho and para, and the two fine structure state configurations, F_1 and F_2, split the N_2^+ population into four distinct classes that are separated on the time scales selected in the present research. The rotational relaxation of ortho-N_2^+ ($X^2\Sigma_g$, $v'' = 0$, $J'' = 6.5$) in collisions with Ar turned out to be much less effective than expected on the basis of simple dynamical and statistical assumptions. This is in contrast to the earlier LIF work by Mahan and O'Keefe [4] that was performed in a Paul trap. Note, however, that in our trap the collision energy is much lower; therefore, details of the long range part of the PES become increasingly important,

as already discussed. In order to unravel the unexpected behavior, the extension of the present experiment to other rotational states and other temperatures is in preparation.

In combination with the well-known LIF experiments, performed with single stored atomic ions such as Be^+, Ba^+, Hg^+, or Mg^+ it is interesting to discuss a similar detection scheme for molecular ions also. Inspection of Fig. 2 reveals that for N_2^+ the cycle of laser excitation, fluorescence, and rotational relaxation is not closed because the initial ion can be lost by charge transfer with Ar. However, the situation is different when the Ar target gas is replaced by He. This leads to a closed scheme and the system may be used to prepare a single molecule spectroscopy experiment. In light of the present results, this system may seem unfavorable not only because of the long lifetime of the N_2^+ (A) state, but also because of the slow rotational relaxation that both lead to a reduction of the LIF signal. However, the use of a second or more diode lasers will help to eventually pump the N_2^+ out of the fine structure or nuclear spin state where it may be "shelved."

Acknowledgements

This work has been funded by the Deutsche Forschungsgemeinschaft under Ge 395/9-1. We thank Dipl. Phys. H. Kalmbach and Dr. W. Paul for technical assistance at the beginning of this experiment.

References

[1] F.J. Grieman, J.C. Hansen, J.T. Moseley, Chem. Phys. Lett. 85 (1982) 53.
[2] A. Carrington, D.R.J. Milverton, P.J. Sarre, Mol. Phys. 35 (1978) 1505.
[3] S. Kato, J.A. de Gouw, C.D. Lin, V. Bierbaum, S.R. Leone, Chem. Phys. Lett. 256 (1996) 305.
[4] B.H. Mahan, A. O'Keefe, J. Chem. Phys. 74 (1981) 5606.
[5] W. Paul, B. Lücke, S. Schlemmer, D. Gerlich, Chem. Phys. 209 (1996) 265; W. Paul, B. Lücke, S. Schlemmer, D. Gerlich, International J. Mass Spectrom. Ion Processes 149 (1995) 373.
[6] A. Sorgenfrei, D. Gerlich, in Molecules and Grains in Space, I. Nenner (Ed.), AIP, Woodbury, NY, 1994, p. 505; D. Gerlich, in Molecules and Grains in Space, I. Nenner, (Ed.), AIP, Woodbury, NY, 1994, p. 489; D. Gerlich, J. Chem. Faraday Trans. 89 (1993) 2199.
[7] G. Herzberg, Molecular Spectra and Molecular Structure. I. Spectra of diatomic Molecules, Krieger, Malabar, 1950.
[8] A. Lofthus, P.H. Krupenie, J. Phys. Chem. Ref. Data 6 (1977) 113.
[9] T.A. Miller, T. Suzuki, E. Hirota, J. Chem. Phys. 80 (1984) 4671.
[10] T. Kuhn, Diplom thesis, Technical University Chemnitz, 1996.
[11] W. Lindinger, F. Howorka, P. Lukas, S. Kuhn, H. Villinger, E. Alge, H. Ramler, Phys. Rev. A 23 (1981) 2319.
[12] D. Smith, N.G. Adams, Phys. Rev. A 23 (1981) 2327.
[13] D. Gerlich, Adv. Chem. Phys. LXXXII (1992) 1.
[14] W. Paul, D. Gerlich, Temperature of Trapped Ions Measured with Spectroscopic Methods, in Proceedings of the 18th International Conference on the Physics of Electronic and Atomic Collisions, Aarhus, 1993.
[15] L.T. Earls, Phys. Rev. 48 (1935) 264.
[16] The laser is smaller in cross section than the cross sectional area explored by the ion cloud. Therefore, an effective area of the ion cloud has to be used for A_{eff} ($=57\ \text{mm}^2$). The effective linewidth for laser excitation is smaller than the Doppler linewidth of the ion cloud, therefore, the latter ($\delta\nu_{\text{Doppler}} \approx$ 500 MHz at $T = 100$ K) has to be used in Eq. 3.
[17] S. Kato, V. Bierbaum, S.R. Leone, Int. J. Mass Spectrom. Ion Processes 149 (1995) 469.
[18] S. Kato, M.J. Frost, V.M. Bierbaum, S.R. Leone, Can. J. Chem. 72 (1994) 625.
[19] M.J. Frost, S. Kato, V.M. Bierbaum, S.R. Leone, J. Chem. Phys. 100 (1994) 6359.
[20] J. Mähnert, H. Baumgärtel, K.-M. Weitzel, J. Chem. Phys. 102 (1995) 180.
[21] D. Gerlich, J. Chem. Phys. 92 (1990) 2377.
[22] D. Gerlich, J. Chem. Phys. 90 (1989) 3574.
[23] M. Quack, Mol. Phys. 34 (1977) 477.
[24] J.H. Langenberg, I.B. Bucur, P. Archirel, Chem. Phys. 221 (1997) 225; P. Archirel, Chem. Phys. 221 (1997) 237; P. Archirel, B. Levy, Chem. Phys. 106 (1986) 51.
[25] D. Gerlich, J. Chem. Faraday Trans. 89 (1993) 2210.